Akt/cAMP-Responsive Element Binding Protein/Cyclin D1 Network: A Novel Target for Prostate Cancer Inhibition in Transgenic Adenocarcinoma of Mouse Prostate Model Mediated by Nexrutine, a *Phellodendron Amurense* Bark Extract

Addanki P. Kumar,[1] Shylesh Bhaskaran,[1] Manonmani Ganapathy,[1] Katherine Crosby,[5] Michael D. Davis,[4] Peter Kochunov,[4] John Schoolfield,[2] I-Tien Yeh,[3] Dean A. Troyer,[3] and Rita Ghosh[1]

Abstract

Purpose: Development of prostate cancer prevention strategies is an important priority to overcome high incidence, morbidity, and mortality. Recently, we showed that Nexrutine, an herbal extract, inhibits prostate cancer cell proliferation through modulation of Akt and cAMP-responsive element binding protein (CREB)–mediated signaling pathways. However, it is unknown if Nexrutine can be developed as a dietary supplement for the prevention of prostate cancer. In this study, we used the transgenic adenocarcinoma of mouse prostate (TRAMP) model to examine the ability of Nexrutine to protect TRAMP mice from developing prostate cancer.

Experimental Design: Eight-week-old TRAMP mice were fed with pelleted diet containing 300 and 600 mg/kg Nexrutine for 20 weeks. Efficacy of Nexrutine was evaluated by magnetic resonance imaging at 18 and 28 weeks of progression and histologic analysis of prostate tumor or tissue at the termination of the experiment. Tumor tissue was analyzed for modulation of various signaling molecules.

Results: We show that Nexrutine significantly suppressed palpable tumors and progression of cancer in the TRAMP model. Expression of total and phosphorylated Akt, CREB, and cyclin D1 was significantly reduced in prostate tissue from Nexrutine intervention group compared with tumors from control animals. Nexrutine also inhibited cyclin D1 transcriptional activity in androgen-independent PC-3 cells. Overexpression of kinase dead Akt mutant or phosphorylation-defective CREB inhibited cyclin D1 transcriptional activity.

Conclusions: The current study shows that Nexrutine-mediated targeting of Akt/CREB–induced activation of cyclin D1 prevents the progression of prostate cancer. Expression of CREB and phosphorylated CREB increased in human prostate tumors compared with normal tissue, suggesting their potential use as prognostic markers.

Prostate cancer is the second leading cause of cancer-related deaths in men and expected to lead to ~27,350 deaths in 2006 (1). African American men have the highest incidence of prostate cancer in the world, whereas Asian men native to their countries who consume a low-fat, high-fiber diet have the lowest risk (2). Epidemiologic studies suggest that a reduced risk of cancer is associated with the consumption of a phytochemical-rich diet that includes fruits and vegetables (3). Evidence suggests that prostate cancer progresses from normal epithelium to proliferative inflammatory atrophy, to low-grade prostatic intraepithelial neoplasia (PIN), and to high-grade PIN that eventually progresses to the more aggressive-metastatic and clinically evident prostate cancer (ref. 4 and references therein). Such preneoplastic lesions have been found in young men in their 20s and are common in men in their 50s (5). However, clinically detectable prostate cancer does not generally manifest itself until the 60s. In addition, the occurrence of precancerous lesions is more prevalent (about 1 in three men) than the incidence of carcinoma (about one in nine men; ref. 6). Therefore, the development of effective strategies for the prevention of early-stage prostate cancer is of utmost importance to ensure quality of life for elderly men. The long latency involved in the development of clinically significant prostate cancer provides plethora of opportunities for intervention, including the use of phytochemicals.

Many components derived from dietary or medicinal plants have been found to possess substantial chemopreventive properties both in rodents and in humans (7). Further, phytochemicals, such as green tea polyphenols, tomato products,

Authors' Affiliations: Departments of [1]Urology, [2]Medicine, and [3]Pathology and [4]Research Imaging Center, University of Texas Health Science Center at San Antonio, San Antonio, Texas and [5]Cell Signaling Technology, Inc., Danvers, Massachusetts

Received 12/18/06; revised 1/21/07; accepted 2/2/07.

Grant support: NIH grants R21 CA 98744 and ACS RSG-04-169-01 (A.P. Kumar) and San Antonio Cancer Institute Cancer Center support grant P30 CA54174.

The costs of publication of this article were defrayed in part by the payment of page charges. This article must therefore be hereby marked *advertisement* in accordance with 18 U.S.C. Section 1734 solely to indicate this fact.

Requests for reprints: Addanki P. Kumar, Department of Urology, University of Texas Health Science Center at San Antonio, 7703 Floyd Curl Drive, San Antonio, TX 78229. Phone: 210-567-5647; Fax: 210-567-6868; E-mail: kumara3@uthscsa.edu.

doi:10.1158/1078-0432.CCR-06-2974

and pomegranate juice, have shown promising activity in human clinical trials (8–16) as part of the treatment regimen. Consistent with this observation, 69% of cancer patients used at least one complementary and alternative medicine therapy as part of their cancer treatment (17). Given the fact that cancer arises due to deregulation of multiple signaling pathways, targeting multiple signaling pathways using a combination of agents or complex botanicals offers an added advantage of providing a synergistic or additive effect (18). These data indicate a potential for developing novel nontoxic agents from plants (phytoceuticals) for successful management of prostate cancer.

Nexrutine is a commercially available herbal extract from *Phellodendron amurense* (*Phellodendron* is "cork tree" in Greek), which is widely used for the treatment of inflammation, gastroenteritis, abdominal pain, and diarrhea (19, 20). The tree is native to Asia and has been reported to contain isoquinoline alkaloids, phenolic compounds, and flavone glycosides (19, 20). Recently, we showed for the first time that Nexrutine inhibits prostate cancer cell proliferation through modulation of Akt and cAMP-responsive element binding protein (CREB)–mediated signaling pathways (21). However, it is unknown if Nexrutine can be developed as a dietary supplement for the prevention of prostate cancer. In this study, we used the transgenic adenocarcinoma of mouse prostate (TRAMP) model to examine the ability of Nexrutine to protect TRAMP mice from developing prostate cancer.

Materials and Methods

Preparation of Nexrutine diet. Nexrutine was provided by Next Pharmaceuticals. For *in vivo* experiments, pelleted diet containing different doses of Nexrutine (300 and 600 mg/kg) was prepared at Dyets, Inc. Stability of Nexrutine in the diet pellets was evaluated every month by thin-layer chromatographic analysis. Briefly, 5 g pelleted diet was extracted with 70% methanol and dried under vacuum. Dried powder was resuspended in water and thin-layer chromatographic was done using dichloromethane and methanol (24:1 w/v) as the solvent systems. The chromatographic profile was observed under UV light. Nexrutine was used as a positive control. The chromatograms of pure Nexrutine and the extracted Nexrutine from the pelleted diet were identical (data not shown).

Transgenic mouse experiments. TRAMP model was developed by prostate-specific expression of SV40 large T antigen using the rat probasin promoter (22, 23). TRAMP mice develop prostate tumors with 100% frequency, in progressive stages that facilitate preclinical studies in the prevention, intervention, and regression setting as shown by various groups, including our own (24–31). TRAMP mice, with a pure C57BL/6 background, were obtained from The Jackson Laboratory. All mice were maintained in a climate-controlled environment with a 12-h light/dark cycle. Diet and water were supplied *ad libitum*. For imaging, animals were anesthetized with ketamine (80 mg/kg i.m.) and scanned in a Siemens 3T TRIO magnetic resonance imaging (MRI) scanner using a receive-only surface coil that was custom built for this experiment to provide a full volumetric coverage of the prostate region. A three-dimensional Fast Low Angle Shot sequence with fat suppression was optimized (TR, 27 ms; TE, 5 ms; and flip angle, 22 degrees) to provide a signal-to-noise ratio of 25 at isotropic spatial resolution of 400 microns and total scan time of ~10 min. Prostate seminal vesicle complex (PSVC) volume was measured using MNI Display program.[6] Following the final MRI scan, animals were euthanized and all organs were collected for further analysis. At necropsy, animals were examined to determine if there were any gross organ abnormalities. Animal care and handling was conducted in accordance with established humane guidelines and protocols approved by the University of Texas Health Science Center at San Antonio's Institutional Animal Care and Use Committee.

Tumor histology. Tumors were weighed, harvested, and fixed in 10% neutral buffered formalin. Tumors were paraffin embedded, sectioned, placed on poly-lysine slides, and stained with H&E to visualize cell nuclei and cytoplasm. Prostate lesions were scored using an established grading system for TRAMP mice (21, 22). Noncancerous lesions were graded as 1, 2, or 3, indicating normal tissue, low PIN, and high PIN, respectively. Grades 4, 5, and 6 indicated well-differentiated, moderately differentiated, and poorly differentiated cancerous lesions, respectively. Images were recorded using a light microscope.

Preparation of extracts and Western blot analysis. Fifty milligrams of prostate tumor or tissue (dorso-lateral) were homogenized in liquid nitrogen and lysed in buffer [50 mmol/L Tris-HCl, 150 mmol/L NaCl, 0.5% NP40, 50 mmol/L NaF, 1 mmol/L $NaVO_4$, 1 mmol/L phenylmethylsulfonyl fluoride, 25 μg/mL leupeptin, 25 μg/mL aprotinin, 25 μg/mL pepstatin, 1 mmol/L DTT (pH 7.4)]. After passing the lysate through a 25-gauge needle, cell debris was removed by centrifugation at 12,000 rpm for 30 min. Nuclear extracts were prepared according to

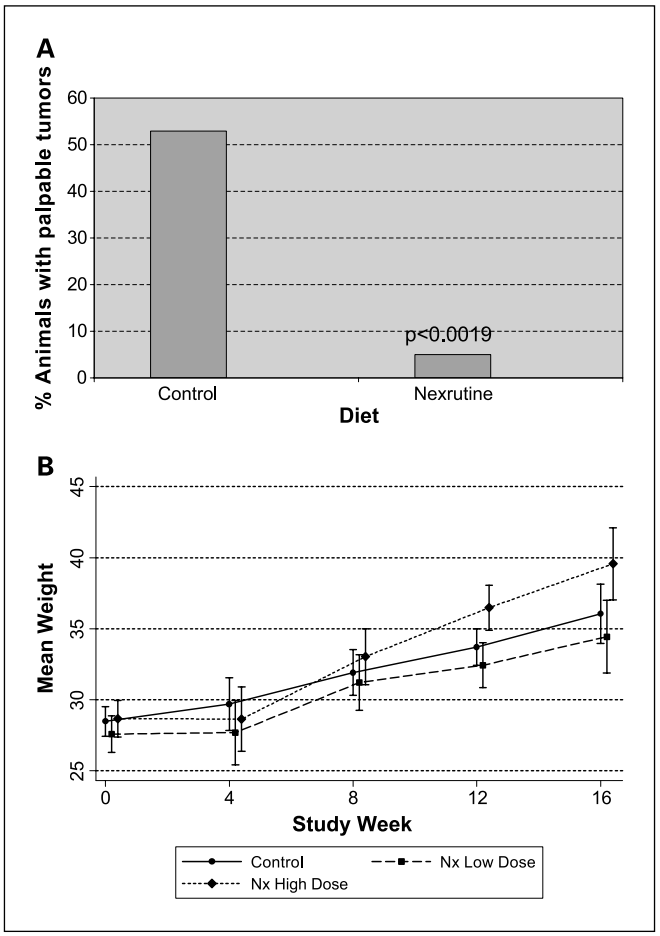

Fig. 1. Effect of Nexrutine on tumor formation in TRAMP mice. Eight-week-old TRAMP mice were fed control or Nexrutine (*Nx*)–containing diet for a total of 20 wks as described in Materials and Methods. Animals were observed for tumors by abdominal palpation (*A*) and body weight changes (*B*) throughout the study. Points, mean body weight in grams as a function of age (in weeks); bars, SE. 0, week 8.

[6] D. MacDonald. Technical report, Mc Connell Brain Imaging Center MNI. MNI Display: Program for Display and Segmentation of Surfaces and Volumes. 1996 (http://www.bic.mni.mcgill.ca/software/Display/Display.html).

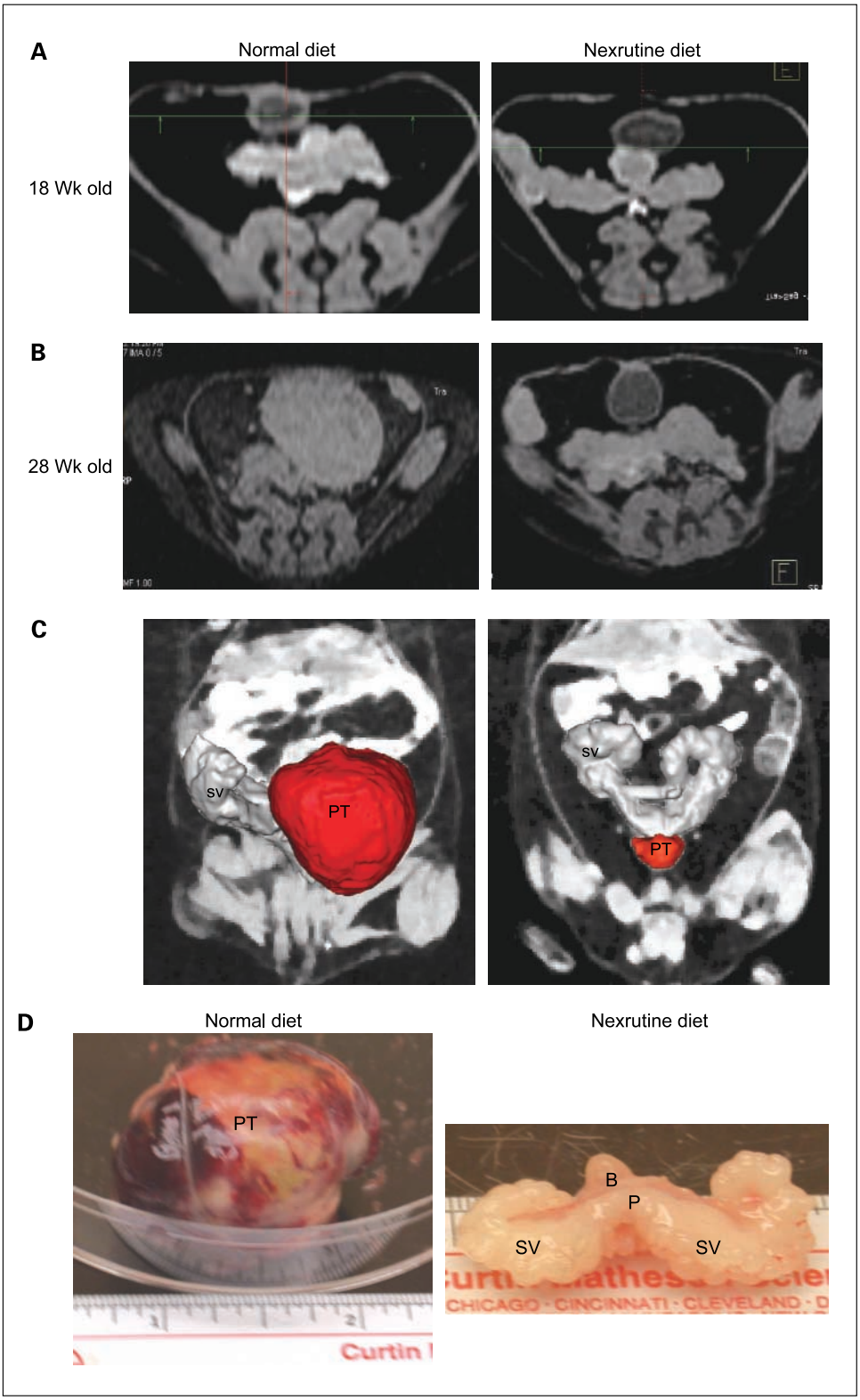

Fig. 2. MRI images of 18- and 28-wk-old TRAMP mice. MRI was used to detect the presence and absence of prostate tumors in response to dietary intervention with Nexrutine. For imaging, animals were anesthetized with ketamine (80 mg/kg i.m.) and scanned in a Siemens 3T TRIO MRI scanner using a receive-only surface coil that was custom built for this experiment to provide a full volumetric coverage of the prostate region. A three-dimensional Fast Low Angle Shot sequence with fat suppression was optimized (TR, 27 ms; TE, 5 ms; and flip angle, 22 degrees) to provide a signal-to-noise ratio of 25 at isotropic spatial resolution of 400 microns and total scan time of ~10 min. PSVC volume was measured using MNI Display program as described in Materials and Methods. *A,* a representative MRI image from an 18-wk-old TRAMP animal on normal and Nexrutine diet for 10 wks. *B,* same animals in (*A*) were imaged at 28 wks of progression (at the time of termination of the study). Representative images show a large prostate tumor in control mice that infiltrated into seminal vesicles, whereas the animal on a Nexrutine-fed diet showed very small prostate with no evidence of tumor. PSVC was determined as described in Materials and Methods using MNI display program. *C,* representative image. *D,* gross appearance of PSVC complex from 28-wk-old TRAMP animal on control or Nexrutine diet, respectively. PT, prostate tumor; P, prostate; SV, seminal vesicles; B, bladder.

the method of Dignam and protein content of the extracts was determined by the method of Bradford as described earlier (32, 33). Equal amounts of extracts were fractionated on a 10% SDS-polyacrylamide gel. Following electrophoresis, proteins were transferred to a nitrocellulose membrane. The blotted membrane was blocked with 5% nonfat dried milk in TBS containing 0.1% Tween 20 and incubated with indicated antibodies (Santa Cruz Biotechnology and Cell Signaling Technology, Inc.) followed by incubation with horseradish peroxidase–conjugated antirabbit IgG antibody (Sigma) in blocking solution. Bound antibody was detected by enhanced chemiluminescence using SuperSignal West Pico chemiluminescent substrate following the manufacturer's directions (Pierce). All the blots were stripped and

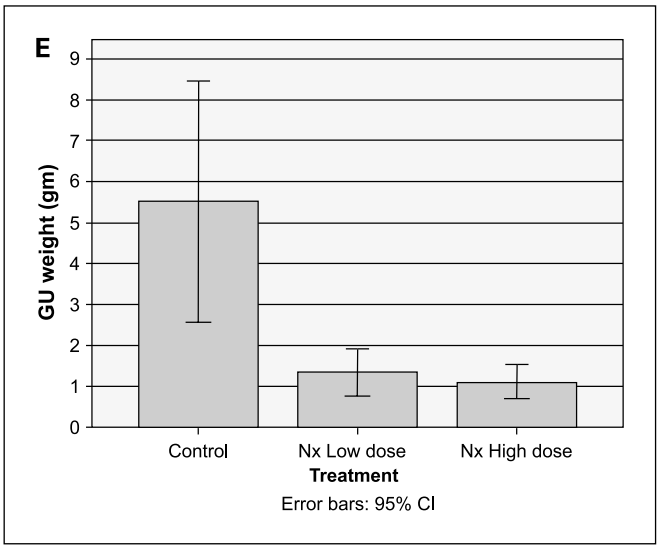

Fig. 2 *Continued. E,* weight of PSVC of TRAMP mice on control and Nexrutine diet at 28 wks. Columns, mean weight in grams; bars, SD.

reprobed with glyceraldehyde-3-phosphate dehydrogenase to ensure equal loading of protein.

Immunohistochemical analysis. Sections from formalin-fixed, paraffin-embedded tissue blocks of prostate were cut and stained with phosphorylated CREB (pCREB; Cell Signaling Technology), phosphorylated Akt (pAkt; Ser^{473}, rabbit monoclonal; 1:50; Cell Signaling Technology), and CREB (Cell Signaling Technology). Proliferation was assessed using the Ki67 (SP6) antibody (Lab Vision). The secondary and tertiary antibodies were biotinylated link and streptavidin horseradish peroxidase (Biocare 4 plus kit, Biocare Medical or Vector Laboratories).

Proliferation and terminal deoxynucleotidyl transferase–mediated dUTP nick end labeling staining in tumors. Proliferation was assessed using the Ki67 (SP6) antibody. The secondary and tertiary antibodies were a biotinylated link and streptavidin horseradish peroxidase (Biocare 4 plus kit). Apoptosis was assessed using *in situ* the terminal deoxynucleotidyl transferase–mediated dUTP nick end labeling (TUNEL) assay, with biotin-16-dUTP (Roche Applied Science) and terminal deoxynucleotidyl transferase (Invitrogen) according to manufacturer's recommendations.

CREB DNA binding activity. CREB DNA binding activity was measured in TRAMP nuclear extracts using TransAM CREB (Active Motif) as described earlier (21). The sequence of the wild-type CREB was 5′-AGAGATTGCCTG**AC**GTCAGAGAGCTAG-3′ (mutated nucleotides shown in bold). Extracts were incubated with CREB consensus oligonucleotide that was immobilized in a 96-well plate. A primary antibody specific for an epitope on the bound and active form of CREB was added followed by subsequent incubation with secondary antibody and developing solution. Following incubation, CREB activity was measured, colorimetrically, at 450 nm. Nuclear extracts prepared from human fibroblast WI-38 cells stimulated with Forskolin (CREB activator) was used as a positive control. For competition experiments, the wells containing immobilized oligonucleotide were preincubated with a 100-fold molar excess of wild-type and mutant oligonucleotide for 30 min before adding the nuclear extract.

Prostate cancer tissue array. Immunohistochemical staining for CREB, pCREB, and pAkt was conducted on a human prostate cancer tissue array containing 15 specimens of different Gleason grades with paired normal prostate. The array was prepared and provided by Dr. Dean Troyer (Department of Pathology, University of Texas Health Science Center, San Antonio, TX). Each specimen was analyzed for immunoreactivity using a 1 to 4+ scoring system for stain intensity and percentage of positive cells. Grading scale for intensity ranged from undetectable signal (1+) to strong signal (4+). The percentage of staining was scored by counting the positive stained cells and total number of cells in four random microscopic fields.

Statistical analysis. Dichotomous measures, such as the presence or absence of (*a*) prostate tumors and (*b*) cancerous lesions with grade of 4 or higher, were evaluated for treatment group differences using Fisher's exact tests. Owing to the small sample size and similarity of outcome frequencies for the low- and high-dose Nexrutine treatment groups, the groups were then combined and compared versus controls using Fisher's exact tests. Because the reduction in tumor frequency was a primary hypothesis of the study, a power analysis was done to determine the likelihood of observing a clinically significant response with the proposed sample size of 15 control and 20 experimental mice. In the population of TRAMP mice, if 50% or more mice receiving the control diet develop prostate tumors, whereas 10% or fewer mice receiving the experimental diet develop prostate tumors, then this difference in tumor rates can be considered clinically significant. This can be detected with the proposed sample size by Fisher's exact test at the 0.05 level with power of 80%. One-way ANOVA was done to determine if there were any significant treatment group mean differences for prostate weights. Post-hoc tests adjusting for the number of comparisons were done to identify group differences if the F test was significant. The weekly mouse weight data were analyzed using mixed-model ANOVA, assuming a first-order autoregressive covariance structure for the repeated effect by week. The mixed-model ANOVA tested for interaction between treatment group and week, as well as the individual main effects and post-hoc comparisons, was done when the estimated treatment group means for a given week were significantly different (determined by F test). Because weight changes were substantial at monthly intervals relative to weekly intervals, the mixed-model ANOVA was done by restricting the data to the baseline, 4-, 8-, 12-, and 16-week measures. For all statistical tests, P values <0.05 were considered significant, with the exception that the test for interaction in the ANOVA model was considered significant if $P < 0.10$. The power analysis was done using PASS 6.0 software. Statistical analyses and graphics were done using SPSS and Stata software.

Results and Discussion

Dietary intervention with Nexrutine suppresses palpable tumors in TRAMP mice. Eight-week-old TRAMP mice (at which time they display high-grade PIN) were randomized into two groups of 10 animals each and fed with AIN-96A pelleted diet containing either 300 or 600 mg/kg Nexrutine. A third group of 15 animals was fed with control diet without Nexrutine. These doses were chosen from a dose escalation xenograft study (data not shown). The ability of Nexrutine to prevent prostate cancer progression was assessed at 18 and 28 weeks of progression by determining the volume of the PSVC using noninvasive MRI. At the termination of the study (28 weeks), the weight of the PSVC was determined and histologic evaluation of the prostate gland and tumor (if present) was carried out. Changes in body weight and food consumption were measured weekly and the experiment was terminated when the animals were 28 weeks old. At the time of necropsy, all other organs, including lungs, liver, and kidney, were collected for histopathologic evaluation.

At the time of termination, 53% of the animals in the control group (n = 15) had palpable tumors. On the other hand, none of the animals in the low-dose group (n = 10) and only 10% of the animals in the high-dose group (n = 10) had palpable tumors. Analysis of these data showed that dietary intervention with Nexrutine significantly suppressed the occurrence of palpable tumors (P = 0.0052, control versus either dose of

Nexrutine). When we combined the data from both experimental dose groups and compared it with the control group, the data reached even greater significance ($P = 0.0019$; Fig. 1A). These data show that Nexrutine intervention decreased palpable tumors, indicating its potential for either reducing tumor incidence and/or increasing latency of tumor development.

Mean body weight changes in response to Nexrutine intervention with respect to age of animals in weeks are shown in Fig. 1B. The mixed-model ANOVA indicated a significant interaction between treatment groups and time ($F = 1.8$; $P = 0.086$), indicating that treatment group mean differences varied by week. No significant differences in the body weight of these animals between control and experimental groups were seen through 8 weeks of dietary intervention ($F = 1.4$ and $P = 0.259$ at 4 weeks of intervention; $F = 1.1$ and $P = 0.346$ at the end of 8 weeks of intervention). Furthermore, Nexrutine treatment produced significant group mean differences ($F = 5.4$ and $P = 0.008$ at 12 weeks; $F = 4.9$ and $P = 0.012$ at 16 weeks). Animals in the high-dose group had a significant increase in body weight compared with the low-dose group, using Bonferroni-adjusted t tests ($P = 0.008$ at 12 weeks; $P = 0.018$ at 16 weeks) with similar results compared with the control group ($P = 0.062$ at 12 weeks; $P = 0.043$ at 16 weeks). Animals in the low-dose group showed no significant difference from control animals in any week. The observed increase in body weight in the high-dose group could not be attributed to differences in food consumption (data not shown). Because the animals in the experimental group did not show significant loss in their body weights, these data indicate nontoxic nature of Nexrutine.

Dietary intervention with Nexrutine retards progression of prostate tumors in TRAMP mice. Volumetric analysis of PSVC at the time of MRI scanning showed that the average PSVC volume varied between 1,025 to 7,000 mm^3 in the control animals ($n = 6$) compared with 700 to 1,600 mm^3 in the treated animals ($n = 6$). MRI analysis data show an ~4-fold increase in the prostate volume in animals on control diet from 18 to 28 weeks. In contrast, animals on the Nexrutine diet, irrespective of the dose, showed ~2-fold increase in the prostate volume during the same period (Fig. 2A and B). PSVC volume measured by MNI display program is shown in Fig. 2C. Following the final imaging, animals were euthanized, all the organs were collected, and wet weight of the PSVC apparatus was determined as described in Materials and Methods (Fig. 2D). As shown in Table 1, mean (with 95% confidence intervals) PSVC weight from animals on control diet ($n = 15$) was ~5.51 g (95% confidence interval, 2.57-8.46). In contrast, the mean weight of PSVC was 1.36 g (95% confidence interval, 0.78-1.95) and 1.11 g (95% confidence interval, 0.69-1.53) from animals on low- and high-dose Nexrutine ($n = 10$ for each dose), respectively. Owing to the heterogeneous variances, a robust ANOVA was done, which indicated significant group mean differences ($F = 9.3$; $P = 0.0023$). Post-hoc comparisons using Games-Howell tests showed that the observed mean differences were significant ($P = 0.024$ and 0.017 between control versus low-dose Nexrutine and control versus high-dose Nexrutine, respectively) but not between low and high dose of Nexrutine. PSVC weight decreased despite 10% of the animals showing palpable tumors, which could be due to heterogeneity of prostate cancer or these may be nonresponders. We believe that the observed palpable tumors (10%) in the high-dose Nexrutine group but not in low dose could be due to heterogeneity of prostate cancer. One would expect a multifold increase in PSVC weight if a palpable tumor was present compared with mice with no palpable tumors; in fact, the one positive high-dose mouse had a PSVC weight of 1.3 g, which was well within the range of other mice without palpable tumors (0.24-1.6 g). Thus, the PSVC weight for the one positive high-dose mouse was not exceptionally high. These data show that animal fed with Nexrutine displayed a significant reduction in the weight of the prostate gland compared with animals on normal diet (Fig. 2E; Table 1).

Histologic evaluation of the prostate tumor/tissue from TRAMP mice fed with control and experimental diet is shown in Fig. 3A. Prostate from control animals showed well-differentiated adenocarcinoma characterized by variable nuclear shape with little or no gland formation. This is consistent with published results using this model (22, 23). In contrast, prostates from animals fed with low-dose Nexrutine exhibited features consistent with high-grade PIN, such as increased variability in nuclear shape with apoptotic and mitotic features (Fig. 3A), whereas prostates from mice fed with high-dose of Nexrutine exhibited pathologic features consistent with the

Table 1. Effect of Nexrutine on wet weight of PSVC in 28-wk-old TRAMP mice

	n	Mean (95% CI)	SD	SE	Minimum	Maximum
Control	15	5.513 (2.568-8.459)	5.319	1.373	0.24	16.80
Nx low dose	10	1.361 (0.775-1.947)	0.819	0.259	0.30	3.40
Nx high dose	10	1.113 (0.694-1.532)	0.586	0.185	0.35	2.20
	P					
Robust F test ($F = 9.3$)	0.0023					
Games-Howell tests						
Control vs Nx low dose	0.0243					
Control vs Nx high dose	0.0168					
Nx Low vs high dose	0.7209					

NOTE: Eight-week-old TRAMP mice were fed with control or Nexrutine-containing diet for a total of 20 wks as described in Materials and Methods. Experiment was terminated when animals were 28 wks old. Weight of the PSVC was determined as described in Materials and Methods. Mean weight in grams of the PSVC weight and the statistical analysis of the data were done as described in Materials and Methods. Abbreviations: Nx, Nexrutine; 95% CI, 95% confidence interval.

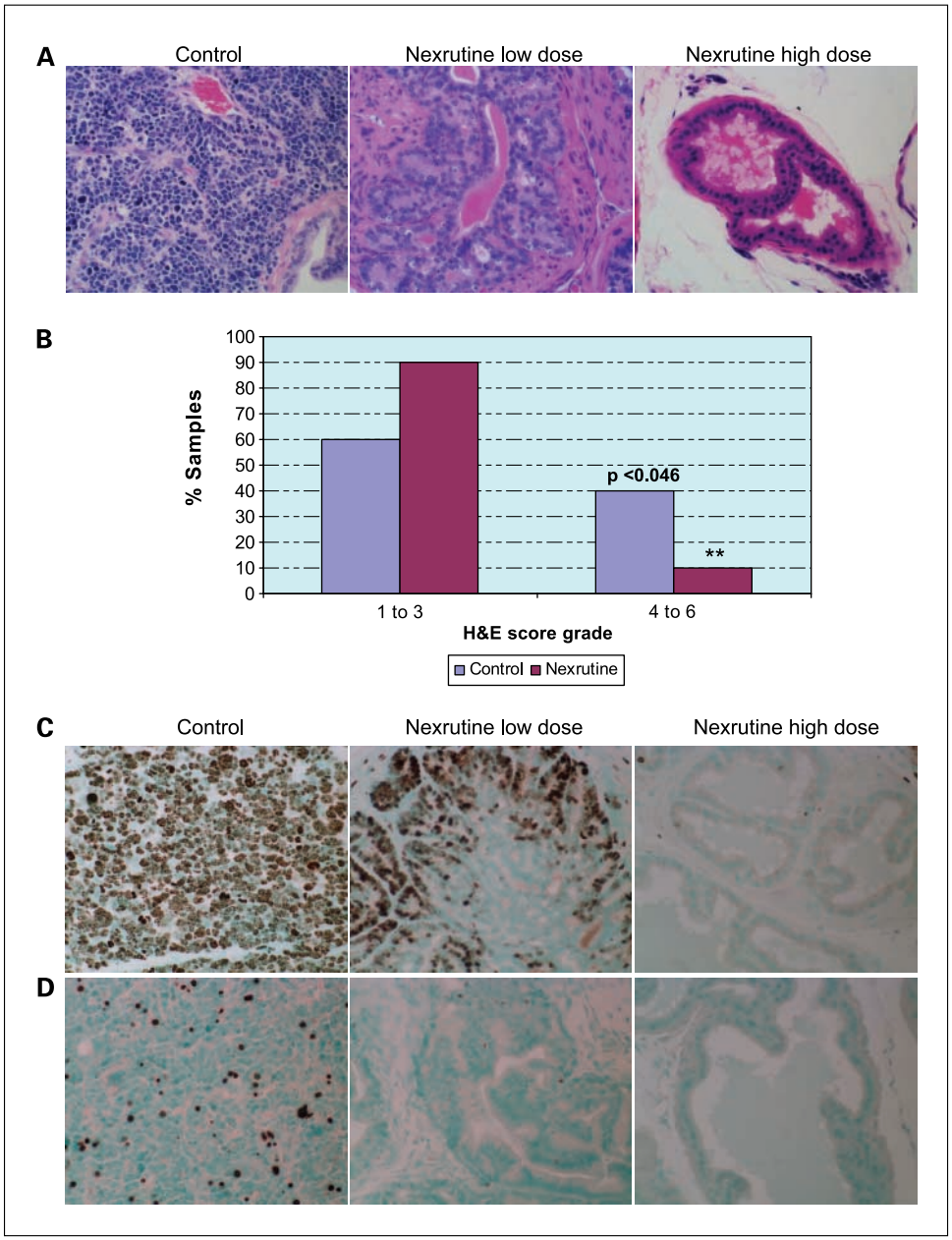

Fig. 3. *A,* histopathologic analysis of prostate or tumor from untreated and treated TRAMP mice. Sections of prostate tissues excised from TRAMP mice were stained with H&E. Histopathologic evaluation of prostate was done on H&E-stained slides as described in Materials and Methods. The prostatic lesions were graded as described earlier on a scale of 1 to 6. Briefly, noncancerous lesions were graded as 1, 2, or 3, indicating normal tissue, low PIN, and high PIN, respectively. Grades 4, 5, and 6 indicated well-differentiated, moderately differentiated, and poorly differentiated cancerous lesions, respectively. Power analysis was done using PASS 6.0 software. Statistical analyses and graphics were done using SPSS and Stata software as described in Materials and Methods. For all statistical tests, P values <0.05 were considered significant. *B,* quantitative analysis of the data. *C,* proliferation of prostate tumor tissues. Paraffin-embedded tissues sections were stained with Ki67 (SP6) antibody to assess proliferation. The secondary and tertiary antibodies were a biotinylated link and streptavidin horseradish peroxidase (Biocare 4 Plus kit). Negative controls were included by omitting the primary antibody or terminal deoxynucleotidyl transferase (for TUNEL). *D,* TUNEL staining in prostate tumor tissues. Apoptosis was assessed in prostate tumor or tissues using the *in situ* TUNEL assay, with biotin-16-dUTP and terminal deoxynucleotidyl transferase.

appearance of normal prostatic epithelium. Cumulative analysis of the data from all the animals indicates that 6 of 15 (40%) control animals and 2 of 18 (10%) animals in the experimental group (low and high dose combined together) were graded as 4 to 6. Eighteen of 20 animals in the experimental group were graded 1 to 3. Statistical analysis of these data indicates that the observed differences are significant ($P = 0.046$; Fig. 3B). These results show that intervention with Nexrutine reduces incidence of adenocarcinoma and retards progression of prostate tumors in TRAMP mice.

Nexrutine reduces proliferation potential of prostate tumors. Previously, we showed that Nexrutine inhibited proliferation of prostate cancer cells by inducing apoptosis (21). Here, we investigated if intervention with Nexrutine would prevent tumor development *in vivo* through inhibition of tumor cell proliferation and induction of apoptosis using Ki67, as a proliferation marker, and TUNEL staining to determine apoptosis. Immunohistochemical analysis indicated that prostates from TRAMP mice fed with control diet are highly proliferative, as indicated by Ki67-positive immunostaining. The number of Ki67-positive cells decreased in Nexrutine dose-dependent manner (Fig. 3C). These *in vivo* data are consistent with our published work in cells showing Nexrutine-inhibited proliferation in prostate cancer cells (21). Prostate tumors from TRAMP mice fed with normal diet also showed more apoptotic cells compared with animals fed with Nexrutine diet as indicated by TUNEL staining (Fig. 3D). There were negligible cells undergoing apoptosis in tissues of animals from Nexrutine treatment (that were graded as normal prostate lesions). In response to Nexrutine treatment *in vivo*, the prostate tissue is normal unlike the cancer cells in our earlier *in vitro* study (21). We did not observe apoptosis in the tissue of animals treated

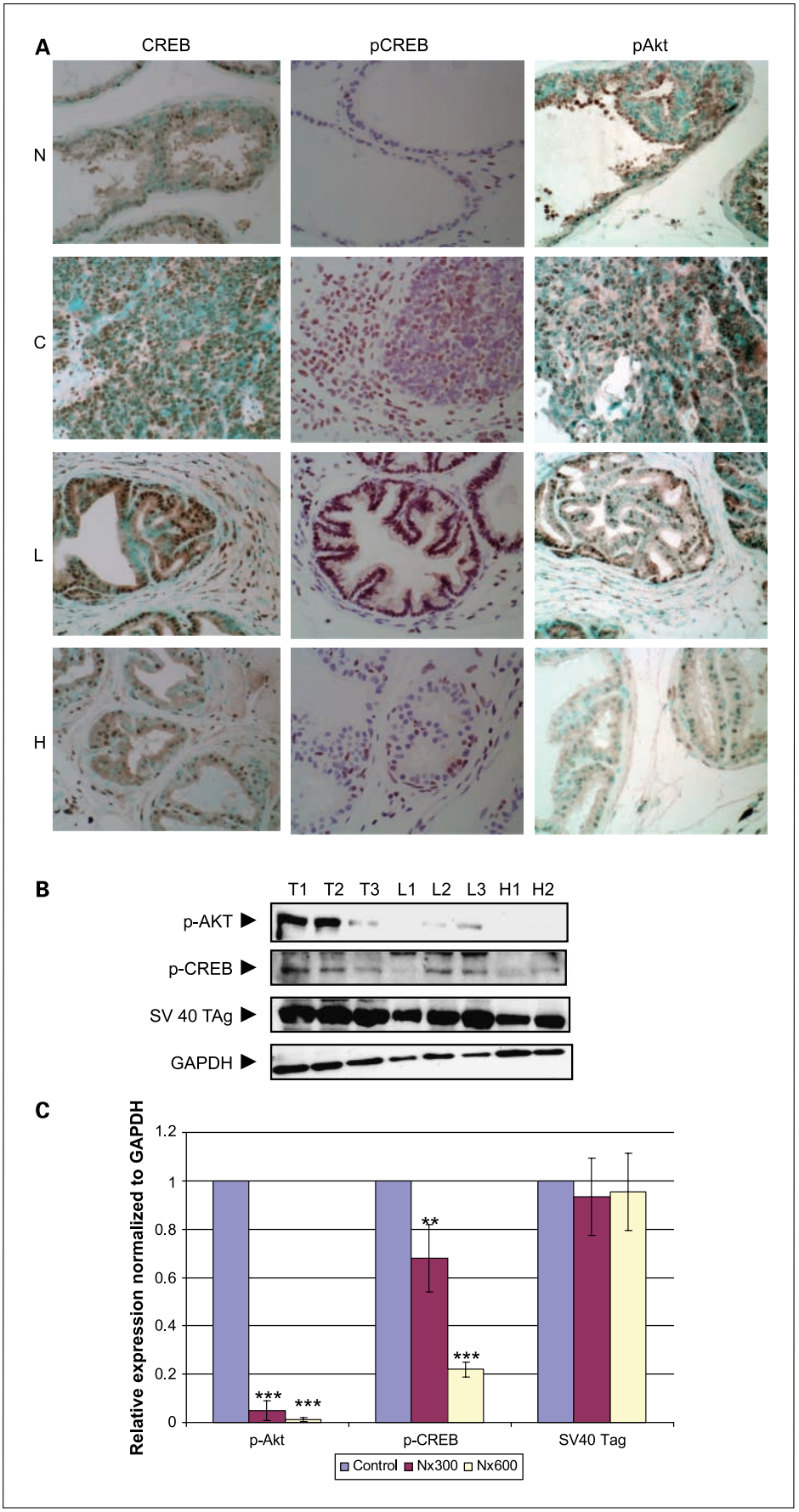

Fig. 4. Immunohistochemical analysis of representative tumors or prostate tissue from 28-wk-old wild-type nontransgenic (*N*), control TRAMP (*C*), or treated, low-dose (*L*) and high-dose (*H*) TRAMP mice. *A,* paraffin-embedded tissues sections were stained with CREB, pCREB, and pAkt antibodies. The antibodies used were at a dilution of 1:100 in PBS and incubated overnight at 4°C. Immune complexes were revealed using a universal secondary antibody (100 μL for 30 min) followed by chromogen. Negative controls were included by omitting the primary antibody. As a control, nontransgenic prostate is also shown. *B,* modulation in the levels of pAkt, pCREB, and SV40 T antigen in TRAMP tissues following Nexrutine treatment. Whole-cell extracts were prepared separately from TRAMP prostate tumors (three individual animals on control diet) or prostate tissue (dorso-lateral from three individual animals on low-dose Nexrutine diet or two different animals on high-dose Nexrutine diet) was used in immunoblot analysis with the indicated antibodies. Equal loading of protein was confirmed with glyceraldehyde-3-phosphate dehydrogenase (*GAPDH*) antibody. Bound antibody was detected by enhanced chemiluminescence using SuperSignal West Pico chemiluminescent substrate following the manufacturer's directions. The blots were imaged using Syngene G Box and quantified using Gene tools software. *C,* graphical representation of the quantified data.

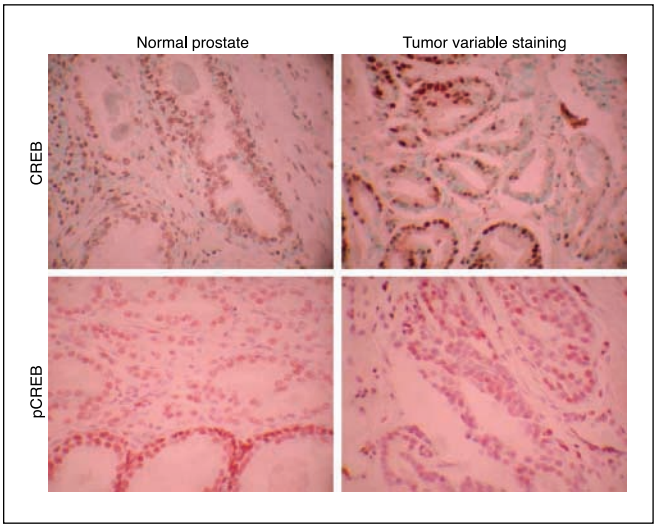

Fig. 5. CREB and pCREB staining in human prostate. Human prostate tissue array containing different grade tumors with paired normal prostate was stained with CREB (*top*) and pCREB (*bottom*). CREB and pCREB were used at a dilution of 1:100 in PBS and incubated overnight at 4°C. Immune complexes were revealed using a universal secondary antibody (100 μL for 30 min) followed by chromogen as described in Materials and Methods. Top, little or no CREB staining in the cancerous tissue; bottom, pCREB expression in normal prostate. Negative controls were included by omitting the primary antibody (data not shown).

with Nexrutine because these were normal or near normal prostate tissue.

***Mechanism of prostate tumor prevention* in vivo.** We have shown that Nexrutine inhibits proliferation and induces apoptosis in prostate cancer cells through modulation of the Akt/CREB signaling pathway (21). We validated these *in vitro* observations *in vivo* by measuring alterations in the expression of pAkt, CREB, and pCREB in triplicate samples from each group of animals (control and low- and high-dose Nexrutine) using immunohistochemistry. Immunoreactivity was scored based on the percentage of stained cells and graded semiquantitatively as 0 (0% stained cells), 1+ (<10% stained cells), 2+ (10-20% stained cells), 3+ (20-50% stained cells), and 4+ (>50% cells stained). Consistent with published literature, pAkt staining was typically localized in the cytoplasm and cell membrane in prostate tumors, whereas CREB staining was predominantly localized in the nuclei of proliferative epithelial cells (Fig. 4A). We also observed increased pAkt and CREB staining during prostate carcinogenesis in TRAMP tissues determined by the intensity of staining (graded 4+). As shown in Fig. 4A, >50% cells from prostate tumors from control animals showed expression of CREB, pCREB, and pAkt. However, prostate tissue from Nexrutine-treated animals showed reduced expression of pAkt, CREB, and pCREB (graded 2+ to 3+). In contrast, very few cells (<10%) showed staining for CREB and pCREB in the prostate from wild-type normal prostate (Fig. 4A, *N*). We confirmed these studies with Western blot analysis using whole-cell extracts prepared from prostate tumors or normal tissue ($n = 3$ from each group). As shown in Fig. 4B, prostate tumors from control group (labeled as T1, T2, and T3 for tumor) expressed high levels of pAkt and pCREB (normalized to glyceraldehyde-3-phosphate dehydrogenase; Fig. 4C). However, in prostate tissue from the treated group (L1, L2, and L3; low), H1 and H2 (high) dose showed significant reduction in the expression of pAkt ($P < 0.01$). Although expression of pCREB was decreased with high-dose Nexrutine treatment, the decrease was less pronounced at low dose compared with pAkt. The observed increase in pAkt staining in prostate tumors from TRAMP mice is consistent with published results (34). To the best of our knowledge, no prior studies have examined the expression of CREB during prostate carcinogenesis, although increased expression of pAkt has been shown in high Gleason grade prostate cancer specimens (35–38). CREB is a nuclear factor that mediates stimulus-induced gene expression through cyclic AMP response element sequence present in the transcriptional regulatory regions of genes (36–39). More than 100 genes involved in various cellular processes, including cell growth, survival, apoptosis, and differentiation, are regulated by CREB (39, 40). Ours is the first report showing the potential involvement of CREB in prostate carcinogenesis. CREB has been shown to (*a*) be overamplified and highly expressed in blast cells from patients with acute myeloid or lymphoid leukemia (41, 42), (*b*) cooperate with oncoprotein to induce cellular transformation (43–45), and (*c*) be involved in survival of melanoma cells, endocrine, and lung tumors (46–48). In addition, transgenic mice overexpressing dominant-negative CREB induces apoptosis in T cells following growth factor stimulation. All these studies implicate CREB as an important factor for cell survival. Our data showing increased expression of CREB in prostate tumors from TRAMP mice is consistent with these published results.

Because TRAMP mice were generated with SV40 large T antigen coupled with probasin promoter (22, 23), we examined whether Nexrutine-mediated effects are a consequence of down-regulation of the PB-Tag transgene using Western blot analysis. As shown in Fig. 4B, PB-Tag and glyceraldehyde-3-phosphate dehydrogenase expression was detected both from control and from treated tumor/tissue obtained from age-matched TRAMP mice. Glyceraldehyde-3-phosphate dehydrogenase levels did not change between control and treated prostatic tissues. These results show that Nexrutine-induced biological effects are due to direct suppression of carcinogenesis and not due to the down-regulation of PB-Tag. Graphical representation of quantification data is shown in Fig. 4C.

CREB and pCREB expression in human prostate tumors. We analyzed the expression of CREB and pCREB in human prostate cancer specimens and normal prostate epithelium using immunohistochemistry. Human prostate cancer tissue arrays containing 15 specimens of different grades and normal tissues were stained for CREB and pCREB. Each specimen was qualitatively analyzed for immunoreactivity (Fig. 5). We found that CREB and pCREB staining was expressed most predominantly in the epithelial nuclei. Of 15 samples analyzed, 9 samples showed positive staining with an intensity of 4+ and other 6 showed 3+. Noteworthy was the heterogeneity observed in the prostate cancer specimens where some of the cancer areas stained stronger (4+) than others. Quantification of the data indicates that >50% of the positively stained cells showed a staining intensity of 4+ and other 50% showed staining intensity of 2+ to 3+. Noteworthy is the observation that tumor cells consistently showed high intensity staining for CREB and pCREB compared with normal epithelium. This is further confirmed in our subsequent studies where we have

examined the staining of CREB and pCREB in the human tissue array containing more samples. These studies show that >50% of the high Gleason (>8/10) grade tumors showed 4+ staining, whereas 75% of low Gleason grade (<7/10) tumors showed 2+ staining.[7] Although the sample size in the current study was small, these observations are very promising and suggest that expression of CREB may be associated with increased tumor grade and therefore greater aggressiveness. Although prostate-specific antigen is used as a marker to detect prostate cancer, it has questionable reliability (49, 50). Due to lack of a molecular marker that can be used to detect a precancerous state or identify which premalignant lesions will develop into invasive prostate cancer, CREB should be pursued further to determine if it can potentially be used as a biomarker. Such studies to relate this to grade, biochemical recurrence, and other clinical features are currently in progress in the laboratory.

Nexrutine inhibits cyclin D1 transcriptional activation. The above results suggest a role for Akt and CREB in prostate carcinogenesis; however, the mechanism through which they promote prostate carcinogenesis is not clear. Activation of CREB by phosphorylation promotes transcription of genes involved in cell proliferation, cell cycle regulation, and inflammation (36–39). In addition, kinases including Akt have been shown to phosphorylate CREB at Ser^{133} (39, 40). Thus, CREB expression in conjunction with other molecular events could affect the progression of prostate cancer. Cyclin D1 is a critical cell cycle regulatory gene involved in G_1-S progression. We analyzed TRAMP prostate tumor/tissue samples for levels of cyclin D1 using Western blot analysis. As shown in Fig. 6A and B, prostate tumors from control diet showed a greater expression of cyclin D1 compared with prostate tissue of treatment group of animals ($P < 0.001$). The promoter region of cyclin D1 contains potential binding site for transcription factor CREB in addition to activator protein 1, Sp1, and nuclear factor-κB (51, 52). Apparently, any of these or some other unidentified factors will be involved in the transcriptional regulation of cyclin D1 in response to Nexrutine. To show this, we examined the effect of Nexrutine on cyclin D1 transactivation using a full-length 1.7 kb promoter (−1,745/+134) of cyclin D1 gene linked to luciferase reporter in PC-3 cells (53). Treatment of cells with Nexrutine resulted in 50% reduction in the promoter activity compared with solvent-treated control (Fig. 6C). These results indicate that Nexrutine can down-regulate cyclin D1 promoter activity. Based on our data showing reduced levels of pAkt, pCREB, cyclin D1, and Akt kinase activity in Nexrutine-treated cells, we reasoned that Akt-mediated activation of CREB regulates cyclin D1 transcriptional activity. We therefore examined the effect of blocking Akt activation using kinase dead Akt mutant expression vector in transient transfection experiments. As shown in Fig. 6C, inactivation of Akt blocked cyclin D1 promoter activity, indicating the importance of Akt signaling in cyclin D1 activation. Further cotransfection of phosphorylation-defective CREB along with cyclin D1 promoter also inhibited cyclin D1 promoter activity. These data collectively indicate an important role for both Akt and CREB in the transcriptional regulation of cyclin D1.

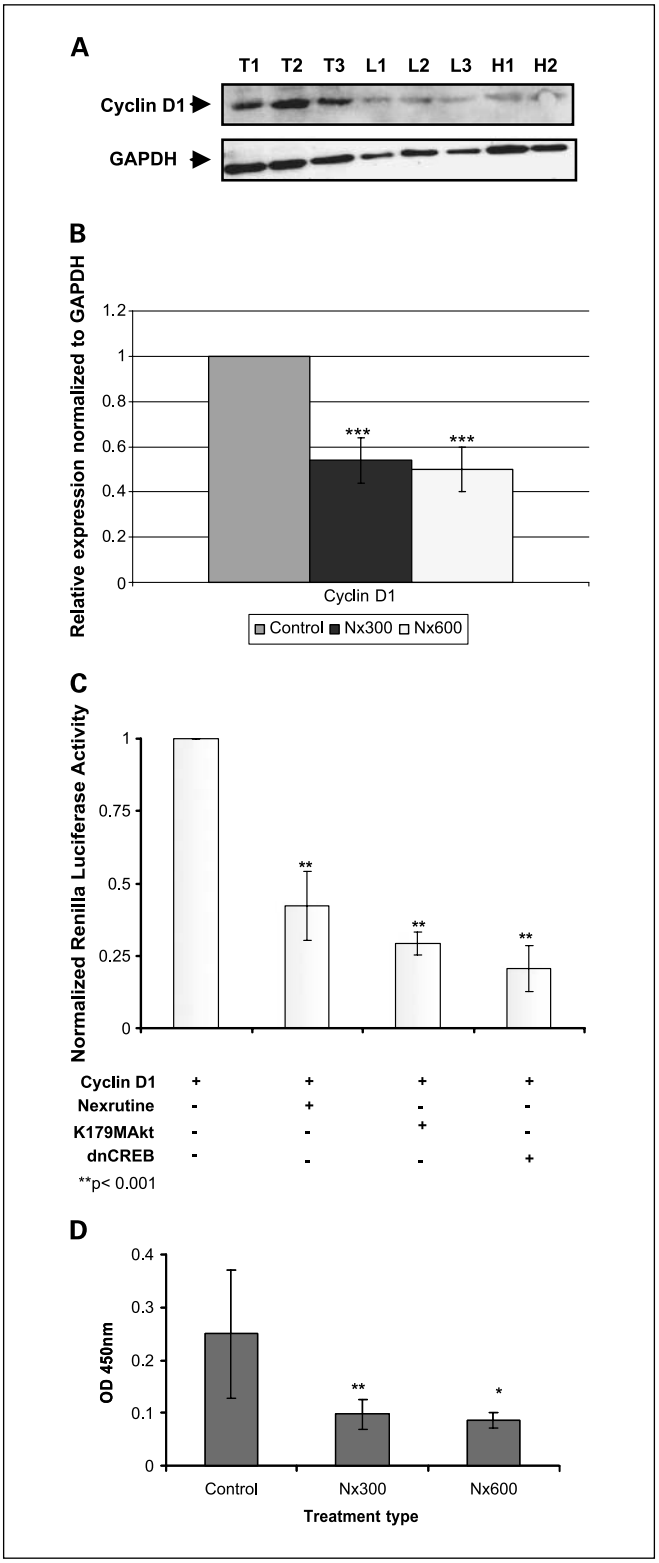

Fig. 6. Nexrutine treatment reduces cyclin D1 levels, cyclin D1 promoter activity, and CREB DNA binding activity. *A,* cyclin D1 levels were determined in TRAMP tissues as described in Fig. 4B. *B,* quantification of Western blot data. *C,* cyclin D1 promoter activity was determined in PC-3 cells. Briefly, either expression plasmids encoding the kinase dead mutant Akt or dominant-negative CREB were transfected with cyclin D1 reporter plasmid into PC-3 cells. *Renilla* luciferase activity was measured as described in Materials and Methods. Columns, average of normalized luciferase activity from three independent transfections; bars, SD. *D,* CREB DNA binding activity was measured in TRAMP nuclear extracts by using TransAM CREB.

[7] A.P. Kumar et al., in preparation.

We measured DNA binding activity of CREB using nuclear extracts prepared from TRAMP prostate tumors. As shown in Fig. 6D, CREB DNA binding activity was reduced in tissues from experimental group of animals compared with that from the control group. This is consistent with our published studies showing a decrease in CREB DNA activity in PC-3 cells following Nexrutine treatment (21). Further, our results showing regulation of cyclin D1 by CREB is also consistent with the published data in lymphocytes (52). These data suggest that Akt/CREB–mediated activation of cyclin D1 plays an important role in the protective effects of Nexrutine in this prostate cancer model. In addition, it is possible that Nexrutine-induced apoptosis in prostate cancer cells proceeds through modulation of CREB as aberrant expression of CREB has been shown to regulate apoptosis (54, 55). Although our results suggest a potential role for Akt in cyclin D1 regulation, participation of other kinases, such as protein kinase A, mitogen-activated protein kinases, Ca^{+2}/calmodulin–dependent protein kinases that are known to activate CREB, cannot be ruled out. Because several growth factors and hormones can activate Akt, Akt/CREB–mediated activation of cyclin D1 may play a role in the development of androgen-independent prostate cancer. Further interactions between AR and CREB through CBP have been shown as a potential mechanism of androgen-independent prostate cancer progression (56). Recently, it was shown that CREB regulates expression of bone matrix proteins, such as osteocalcin and sialoprotein in prostate cancer cells (57). Constitutive activation of Src-mitogen-activated protein kinase/extracellular signal-regulated kinase kinase-1-2-extracellular signal-regulated kinase-1/2-CREB signaling pathway is associated with the androgen-independent phenotype (58). Thus, inhibition of such critical signaling network to prevent prostate cancer progression with a cost-effective nontoxic herbal supplement is a highly significant finding. An added advantage of Nexrutine is that it has a good safety record in humans and is biologically active in human test subjects. The Living Longer Clinic (Cincinnati, OH) conducted a 288-subject open-label, single-center study to test Nexrutine as a potential analgesic. These subjects were given Nexrutine (one to two capsules thrice daily). Two hundred fifty-five (88%) of the subjects reported beneficial effects of Nexrutine, including reduction in pain and/or inflammation, whereas the remainder reported no improvement.[8] To date, the exact nature of the biologically active component(s) in this herbal extract has not been elucidated. Additional studies are currently being carried out in our laboratory to identify and characterize the biologically active principle of Nexrutine and the precise molecular pathways involved in its anticancerous activity. The results of these and future studies with Nexrutine may yield an important addition to the weak therapeutic armamentarium that exists for the treatment of prostate cancer and perhaps other cancers.

[8] http://www.npicenter.com/anm/anmviewer.asp?a=13847

Acknowledgments

We thank Dr. Bob Garrison (Next Pharmaceuticals, Irvine, CA) for kindly providing Nexrutine for this work; Drs. Alex Toker (Beth Israel Deaconess Medical Center, Boston, MA) and Richard Pestell (Thomas Jefferson University, Philadelphia, PA) for Akt expression and cyclin D1 promoter constructs, respectively; Dr. Ian M. Thompson (Department of Urology, University of Texas Health Sciences Center, San Antonio, TX) for reviewing the manuscript; and Marlene Sosa and Javier Esparza for providing technical assistance.

References

1. Jemal A, Siegel R, Ward E, et al. Cancer statistics. CA Cancer J Clin 2006;56:106–30.
2. Yip I, Heber D, Aronson W. Nutrition and prostate cancer. Urol Clin North Am 1999;26:403–11.
3. Chan JM, Gann PH, Giovannucci EL. Role of diet in prostate cancer development and progression. J Clin Oncol 2005;23:8152–60.
4. Kelloff GJ, Lippman SM, Dannenberg AJ, et al. Progress in chemoprevention drug development: the promise of molecular biomarkers for prevention of intraepithelial neoplasia and cancer—a plan to move forward. Clin Cancer Res 2006;12:3661–97.
5. Dunsmuir WD, Hrouda D, Kirby RS. Malignant changes in the prostate with ageing. Br J Urol 1998; 82:47–58.
6. Shen CA, Shen MM. Molecular genetics of prostate cancer. Genes Dev 2001;14:2410–34.
7. Surh YJ. Cancer chemoprevention with dietary phytochemicals. Nat Rev Cancer 2003;3:768–80.
8. Albrecht M, Jiang W, Kumi-Diaka J, et al. Pomegranate extracts potently suppress proliferation, xenograft growth, and invasion of human prostate cancer cells. J Med Food 2004;7:274–83.
9. Bettuzzi S, Brausi M, Rizzi F, Castagnetti G, Peracchia G, Corti A. Chemoprevention of human prostate cancer by oral administration of green tea catechins in volunteers with high grade prostate intraepithelial neoplasia, a preliminary report from a one-year proof-of principle study. Cancer Res 2006;66:1234–40.
10. Birrell MA, McCluskie K, Wong S, Donnelly LE, Barnes PJ, Belvisi MG. Resveratrol an extract of red wine inhibits lipopolysaccharide induced airway neutrophilia and inflammatory mediators through an NFκB B independent mechanism. FASEB J 2005;19:840–1.
11. Choan E, Segal R, Joinker D, et al. A prospective clinical trial of green tea for hormone refractory prostate cancer, an evaluation of the complementary and alternative therapy approach. Urol Oncol 2005;23:108–13.
12. Clinton SK. Tomatoes or lycopene: a role in prostate carcinogenesis. J Nutr 2005;135:2057–9S.
13. Kirsh VA, Mayne ST, Peters U, et al. A prospective study of lycopene and tomato products intake and risk of prostate cancer. Cancer Epidemiol Biomarkers Prev 2006;15:92–8.
14. Pantuck AJ, Leppert JT, Zomorodian N, et al. Phase II study of pomegranate juice for men with rising prostate specific antigen following surgery or radiation for prostate cancer. Clin Cancer Res 2006;12:4018–26.
15. Pianetti S, Guo S, Kavanagh KT, Sonenshein GE. Green tea polyphenol epigallocatechin-3 gallate inhibits HER-2/*neu* signaling, proliferation, and transformed phenotype of breast cancer cells. Cancer Res 2002;62:652–5.
16. Singh AV, Franke AA, Blackburn GL, Zhou JR. Soy phytochemicals prevent orthotopic growth and metastasis of bladder cancer in mice by alteration of cancer cell proliferation and apoptosis and tumor angiogenesis. Cancer Res 2006;66:1851–8.
17. Nahin RL, Straus SE. Research into complementary alternative medicine: problems and potential. Br Med J 2006;322:161–4.
18. McCarty MF. Targeting multiple signaling pathways as a strategy for managing prostate cancer: multifocal signal modulation therapy. Integr Cancer Ther 2004;3: 349–80.
19. Mori H, Fuchigami M, Inoue N, et al. Principle of the bark *Phellodendron amurense* to suppress the cellular immune response: effect of *Phellodendron* on cellular and humoral immune response. Planta Med 1995;61: 45–9.
20. Cuellar MJ, Giner RM, Recio MC, Manez S, Rios JL. Topical anti-inflammatory activity of some Asian medicinal plants used in dermatological disorders. Fitoterapia 2001;72:221–9.
21. Garcia GE, Arevalo N, Bhaskaran S, Gupta A, Kyprianou N, Kumar AP. Akt and CREB mediated prostate cancer cell proliferation inhibition by Nexrutine® a *Phellodendron amurense* extract. Neoplasia 2006;8: 523–33.
22. Gingrich JR, Barrios RJ, Foster BA, Greenberg NM. Pathologic progression of autochthonous prostate cancer in the TRAMP model. Prostate Cancer Prostatic Dis 1999;2:70–5.
23. Gingrich JR, Barrios RJ, Morton RA, et al. Metastatic prostate cancer in transgenic mouse. Cancer Res 1996;56:4096–102.
24. Gupta S, Adhami VM, Subbarayan M, et al. Suppression of prostate carcinogenesis by dietary supplementation of celecoxib in transgenic adenocarcinoma of the mouse prostate model. Cancer Res 2004;64:3334–43.
25. Gupta S, Hastak K, Ahmad N, Lewin JS, Mukhtar H. Inhibition of prostate carcinogenesis in TRAMP mice by oral infusion of green tea polyphenols. Proc Natl Acad Sci U S A 2001;98:10350–5.
26. Gupta S, Ahmad N, Marengo SR, MacLennan GT, Greenberg NM, Mukhtar H. Chemoprevention of prostate carcinogenesis by α-difluoromethylornithine in TRAMP mice. Cancer Res 2000;60:5125–33.
27. McCabe MT, Low JA, Daignault S, Imperiale MJ, Wojno KJ, Day ML. Inhibition of DNA methyltransferase activity prevents tumorigenesis in a mouse model of prostate cancer. Cancer Res 2006;66:385–92.

28. Mentor-Marcel R, Lamartiniere CA, Eltoum IA, Greenberg NM, Elgavish A. Dietary Genistein improves survival and reduces expression of osteopontin in the prostate of transgenic mice with prostatic adenocarcinoma (TRAMP). J Nutr 2005;135: 989–95.

29. Mentor-Marcel R, Lamartiniere CA, Eltoum I-E, Greenberg NM, Elgavish A. Genistein in the diet reduces the incidence of poorly differentiated prostatic adenocarcinoma in transgenic mice (TRAMP). Cancer Res 2001;61:6777–82.

30. Wechter WJ, Leipold DD, Murray DE, et al. E-7869 (R-flurbiprofen) inhibits progression of prostate cancer in the TRAMP mouse. Cancer Res 2001;60: 2203–8.

31. Garcia GE, Wisniewski H-G, M Scott Lucia, et al. 2-Methoxyestradiol (2-ME) inhibits prostate tumor development in transgenic adenocarcinoma of mouse prostate (TRAMP): role of TNFα-stimulated gene 6 (TSG-6). Clin Cancer Res 2006;12:980–8.

32. Kumar AP, Garcia GE, Slaga TJ. 2-Methoxyestradiol blocks cell-cycle progression at G_2/M phase and inhibits growth of human prostate cancer cells. Mol Carcinog 2001;31:111–24.

33. Kumar AP, Garcia GE, Ghosh R, Rajnarayanan RV, Alworth WL, Slaga TJ. 4-Hydroxymethoxybenzoic acid methyl ester (HMBME): a curcumin derivative targets Akt/NFκB cell survival signaling pathway: potential for prostate cancer management. Neoplasia 2003;5:255–66.

34. Shukla S, MacLennan GT, Marengo SR, Resnick MI, Gupta S. Constitutive activation of PI3K-Akt and NFkB during prostate cancer progression in autochthonous transgenic mouse model. Prostate 2005;64: 224–39.

35. Malik SN, Brattain M, Ghosh PM, et al. Immunohistochemical demonstration of phospho Akt in high Gleason grade prostate cancer. Clin Cancer Res 2002;8:1168–71.

36. Mary B, Montminy M. Transcriptional regulation by the phosphorylation-dependent factor CREB. Nat Rev Mol Cell Biol 2001;2:599–609.

37. Du K, Montminy M. CREB is a regulatory target for the protein kinase Akt/PKB. J Biol Chem 1998;273: 32377–9.

38. Conkright MD, Montminy M. CREB: the unindicted cancer co-conspirator. Trends Cell Biol 2005;15:457–9.

39. Okuno H and Bito H. Creb 1. UCSD-Nature Molecules Pages 2006; doi:10.1038/mp.a000690.01.

40. Okuno H and Bito H. Creb 1. Afcs-Nature Molecules Pages 2006; doi:10.1038/mp.a000690.01.

41. Shankar DB, Sakamoto KM. The role of cyclic-AMP binding protein (CREB) in leukemia cell proliferation and acute leukemias. Leuk Lymphoma 2004;45:265–70.

42. Shankar DB, Cheng JC, Kinjo K, et al. The role of CREB as a proto-oncogene in hematopoiesis and in acute myeloid leukemia. Cancer Cell 2005;7:351–62.

43. Zucman J, Delattre O, Desmaze C, et al. EWS and ATF-1 gene fusion induced by t (12;22) translocation in malignant melanoma of soft parts. Nat Genet 1993; 4:341–5.

44. Schaefer KL, Brachwitz K, Wai DH, et al. Expression profiling of t(12;22) positive clear cell sarcoma of soft tissue cell lines reveals characteristic up-regulation of potential new marker genes including ERBB3. Cancer Res 2004;64:3395–405.

45. Olsen RJ, Hinrichs SH. Phosphorylation of the EWS IQ domain regulates transcriptional activity of the EWS/ATF1 and EWS/FLI1 fusion proteins. Oncogene 2001;20:1756–64.

46. Melnikova VO, Mourad-Zeidan AA, Lev DC, Bar-Eli M. Platelet-activating factor mediates MMP-2 expression and activation via phosphorylation of cAMP-response element-binding protein and contributes to melanoma metastasis. J Biol Chem 2006;281:2911–22.

47. Jean D, Harbison M, McConkey DJ, Ronai Z, Bar-Eli M. CREB and its associated proteins act as survival factors for human melanoma cells. J Biol Chem 1998; 273:24884–90.

48. Rosenberg D, Groussin L, Jullian E, Pelemoine K, Bertagna X, Bertherat J. Role of PKA-regulated transcription factor CREB in development and tumorigenesis of endocrine tissues. Ann N Y Acad Sci 2002; 968:65–74.

49. Thompson IM, Ankerst DP, Chi C, et al. Operating characteristics of prostate-specific antigen in men with an initial PSA level of 3.0 ng/mL or lower. JAMA 2005;294:66–70.

50. Tricolli JV, Schoenfeldt M, Conley BA. Detection of prostate cancer and predicting progression: current and future diagnostic markers. Clin Cancer Res 2004; 10:3943–53.

51. Sabbah M, Courilleau D, Mester J, Redcuilh G. Estrogen induction of cyclin D1 promoter involvement of a cAMP response like element. Proc Natl Acad Sci U S A 1999;96:11217–22.

52. White PC, Shore AM, Clement M, et al. Regulation of cyclin D2 and the cyclin D2 promoter by promoter kinase A and CREB in lymphocytes. Oncogene 2006; 25:2170–80.

53. Albanese C, Johnson J, Watanabe G, et al. Transforming $p21^{ras}$ mutants and c-Ets2 activate cyclin D1 promoter through distinguishable regions. J Biol Chem 1995;270:23589–97.

54. Dworet JH, Meinkoth JL. Interference with cAMP response element binding protein (CREB) stimulates apoptosis through aberrant cell cycle progression and checkpoint activation. Mol Endocrinol 2006;20: 1112–20.

55. Saeki K, You A, Suzuki E, Yazaki Y, Takaku F. Aberrant expression of cAMP-response-element-binding protein ('CREB') induces apoptosis. Biochem J 1999; 343:249–55.

56. Debes JD, Comuzzi B, Schmisth LJ, Dehm SM, Culig Z, Tindall DJ. p300 regulates androgen receptor-independent expression of prostate-specific antigen in prostate cancer cells treated chronically with interleukin-6. Cancer Res 2005;65:5965–73.

57. Huang WC, Xie Z, Konaka H, Sodek J, Zhau HE, Chung LW. Human osteocalcin and bone sialoprotein mediating osteomimicry of prostate cancer cells: role of cAMP-dependent protein kinase A signaling pathway. Cancer Res 2005;65:2303–13.

58. Unni E, Sun S, Nan B, et al. Changes in androgen receptor nongenotropic signaling correlate with transition of LNCaP cells to androgen independence. Cancer Res 2004;64:7156–8.

Clinical Cancer Research

Akt/cAMP-Responsive Element Binding Protein/Cyclin D1 Network: A Novel Target for Prostate Cancer Inhibition in Transgenic Adenocarcinoma of Mouse Prostate Model Mediated by Nexrutine, a *Phellodendron Amurense* Bark Extract

Addanki P. Kumar, Shylesh Bhaskaran, Manonmani Ganapathy, et al.

Clin Cancer Res 2007;13:2784-2794.